FACTA UNIVERSITATIS (NIŠ)
SER.: ELEC. ENERG. vol. 16 April 2003, 1-23

Electromagnetic Methods in Nondestructive Testing of Materials

Konstanty M. Gawrylczyk

Invited Paper

Abstract: The article deals with progress in electromagnetic methods used for quality evaluation of conducting materials. The term "electromagnetic methods" covers the following areas: magneto-inductive methods, magnetic leakage flux probe method, magnetometer principle and eddy-current methods. For the aim of numerical cracks recognition the sensitivity analysis with finite elements was shown.

Keywords: Nondestructive testing of materials, finite element method, sensitivity analysis.

1 Introduction

50 years ago Ph.D.F.Förster founded his institute. The history of early systems for nondestructive testing combines closely to the company history [3].

While examining the magnetic properties of metals in 1937, Friedrich Förster discovers the effect of the earth's magnetic field on the magnetic coil of the test setup. He starts with the development of highly sensitive measuring devices for magnetic fields. The objective was the development of equipment suitable for use in industry. The research work of Dr. Förster was presented to various bodies as well as exhibitions and trade fairs. For the scientific foundation of electromagnetic test methods Dr. Friedrich Förster

Manuscript received November 11, 2002

Tke author is with Technical University of Szczecin Sikorskiego 37 PL-70-310 Szczecin, Poland(e-mail: kmg@ps.pl).

was awarded in 1957 the Victor de Forest Award. The method is publicized by Robert C. McMaster, USA 1959, in the standard work for nondestructive test methods. The first industrial implementations came in sixties. Italian factory used his 'Turbotest' leakage flux installation for testing hot rolled tubes for petrochemical use. The equipment of Förster was used in space exploration since 1963, as magnetic field measuring device was installed in an satellite. There was even a Förster probe on the moon. In 1992 the NASA gave its highest award to F.Förster for his work. As one of the first eddy current units, in the early seventies, Saarstahl AG integrates an hot wire testing unit in its wire rolling mill. To specify the quality characteristics of hot-rolled, seamless steel tubes, Mannesmann S.A. Brazil, have been using since 1996 a highly modern multi-test block. In 1998, a similar leakage flux test unit was incorporated in Japan.

2 Areas of Electromagnetic Methods

2.1 Magneto-inductive methods

The feeding frequency covers the band from a few Hz to approx. 1000 Hz. The absolute coils are usually used to determine integral, technological material properties, such as grain structure, hardness, case-hardening depth and layer thickness. It is possible to investigate the core and surface selectively by varying the frequency. For diverse tasks the excitation may be with several frequencies (serial or simultaneous).

2.2 Magnetic leakage flux probe method

The feeding frequency is very low in this case, even the DC-field may be applied. This method fits for testing of tubes and steel bars with round cross-sections. The high-energy alternating magnetic flux concentrates at the material surface and is thus particularly suitable for detection of small surface flaws upwards of a depth of 0.1 mm. Two rotating yokes (Fig.1) generate the magnetic flux locally. The integrated magnetic field sensors detect the leakage flux emerging at the flaws.

The DC field leakage-flux method allows the entire material cross-section to be magnetized and thus permits testing for flaws on the outer and inner surfaces of the tube. Detectability of internal flaws decreases with increasing wall thickness. The magnetic flux is built up in a circular array with two rotating yokes for detection of longitudinal flaws. Co-rotating magnetic field sensors detect the leakage flux emerging at the flaws.

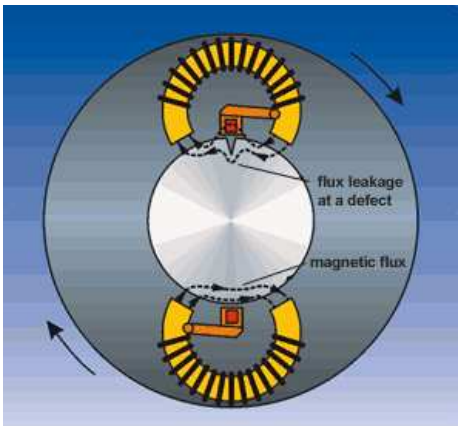

Fig. 1. Magnetic flux leakage method.

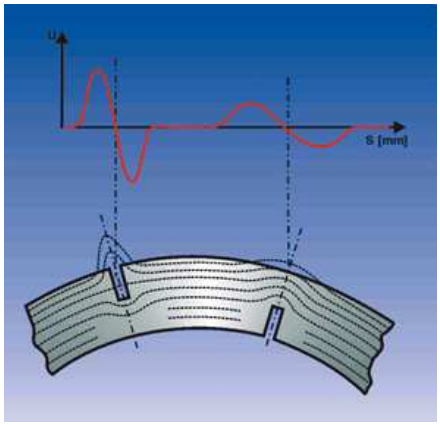

Fig. 2. The signals of inner and outer defect.

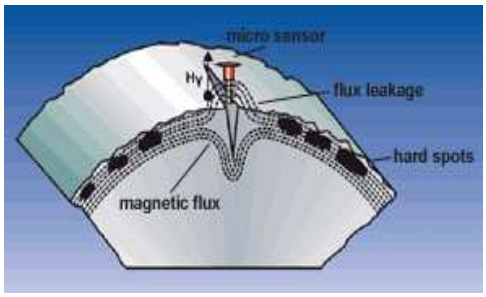

Fig. 3. Magnetizing of material nearby crack.

The magnetic flux is generated by two stationary all-round coils arranged in the longitudinal direction for detection of transverse-oriented flaws. Several magnetic field sensors in a stationary array on the circumference detect the emerging leakage flux.

2.3 Magnetometer principle

This passive, highly sensitive magnetic field sensors are used for the measurement of smallest magnetic fields and magnetic field gradients on earth and in space. Magnetic field of the earth interferences with iron objects. The sensor measures magnetic field gradients. Dipole evaluation signals are the classical result.

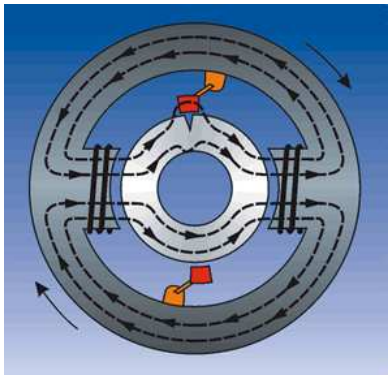

Fig. 4. Detection of radial flux distortion.

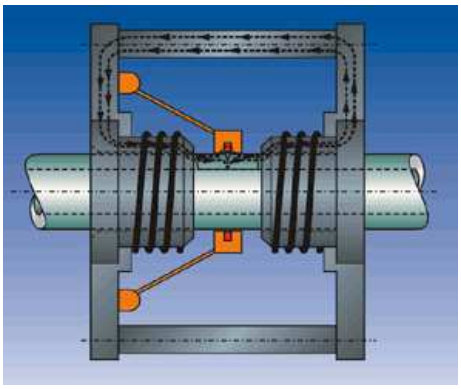

Fig. 5. Detection of longitudinal flux distortion of the flaw.

2.4 Metal detection using the eddy current principle

The sensor generates with one or two frequencies an electromagnetic field. This field is used for the detection of hidden metal objects, even objects with very low metal content. All metals can be detected. Object detection with eddy current method: the active detection sensor of this technology is generating an electromagnetic field. This causes eddy currents in the object to be detected. These eddy currents generate a secondary electromagnetic field which is detected and evaluated by receiver sensor.

2.5 Magnetic leakage flux probe method

2.6 Eddy-current methods

Widespread methods which conventionally cover the frequency band up to approx. 10 MHz with differential coils and which are used for testing for surface and inner flaws.

2.7 Magnetic leakage flux probe method

Semi-finished products, such as wires, bars and tubes, are tested for local flaws in the form of cracks and holes by encircling through-type coils. The surface of semi-finished products or components is scanned with scanning probes. This allows maximum flaw resolution.

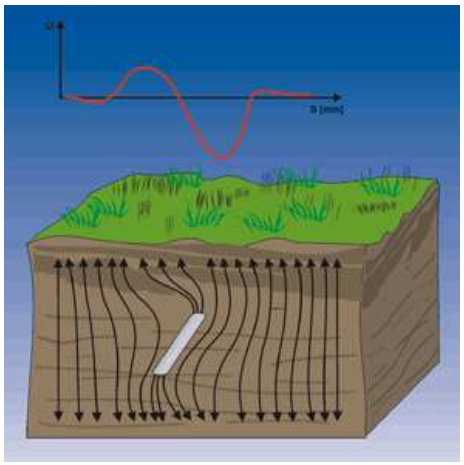

Fig. 6. Earth field interferences by iron objects.

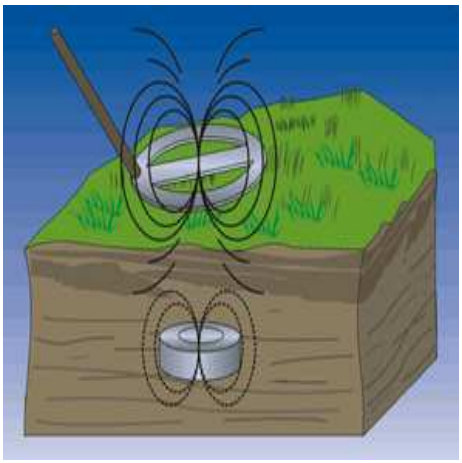

Fig. 7. Conducting object detection with eddy-currents.

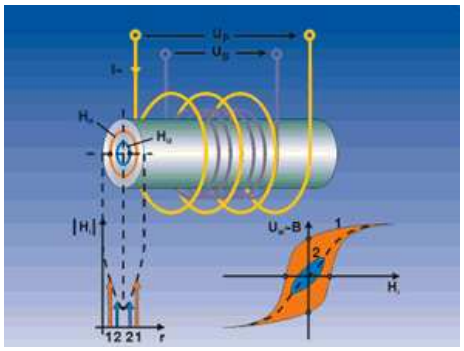

Fig. 8. Testing of bars and tubes.

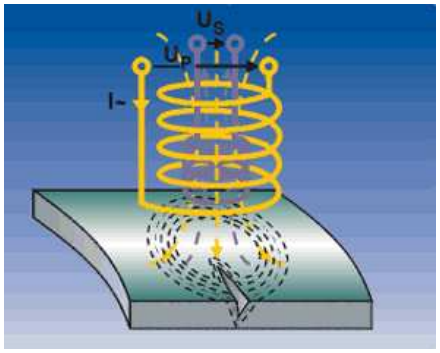

Fig. 9. Testing of surfaces.

3 Eddy Current Basics

The meaning of lift-off effects is for simple probes of great importance. The signal decreases very fast and the distinction of cracks may be impossible. Eddy currents are alternating electrical currents, usually high frequency, which can be induced to flow in any metallic section. The feeding frequency, and adequate penetration depth of eddy- currents, should be adapted to expected cracks. The flow pattern of currents is disturbed by cracks or other discontinuities in the metal. Eddy current flow patterns are either circumferential, using encircling or concentric coil configurations, or a tangential or loop pattern when using a surface or pancake coil configuration. Eddy currents develop their own magnetic fields, detectable by electromagnetic

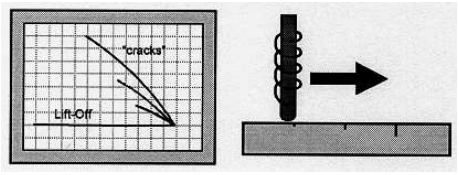

Fig. 10. Effecting of lift off in output signals.

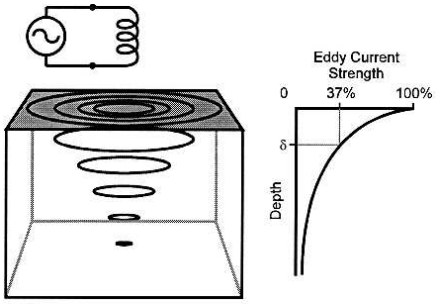

Fig. 11. Penetration depth of eddy-currents.

means. A crack or flaw in the material affects the flow pattern which, in turn, affects its associated magnetic field. This change is detected by a suitable search coil arrangement. Search coils are usually wound in the form of a differential transformer, with the primary or excitation winding being fed from an oscillator. Two secondary windings observe the eddy current effects at displaced sections of the material under test, and automatically compare the cross-sections for any differences which may occur.

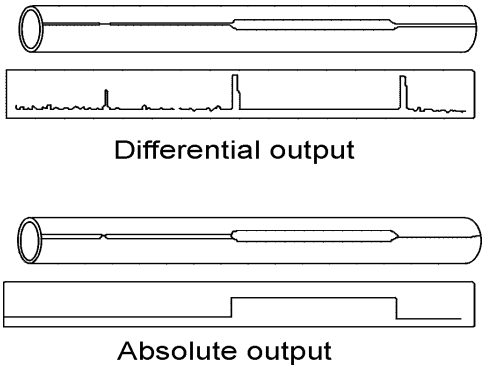

Fig. 12. Output signals of different eddy-current transducers [4].

The obvious limitation of this form of inspection is that no difference in cross-section occurs if a defect is continuous for the material's entire length. In practice, most defects are fairly intermittent in nature, but where it is necessary to detect 'absolute' type defects, then it is possible to augment the differential windings with an extra facility known as an absolute channel. Absolute channels on tube factories are used mainly to detect open seam conditions. When testing ferromagnetic materials, magnetic polariz-

ing assemblies are employed, principally to reduce permeability to a low and constant factor. In these circumstances, eddy current signals may sometimes be influenced by magnetic flux patterns that develop around discontinuities. Most eddy current test units analyze signals for amplitude, phase relationship and frequency patterns and are able to automatically discern flaw signals from noise created by vibration and dimensional and metallurgical variations. These filtering techniques enable higher sensitivities to be achieved, but care has to be taken to ensure that the same signal processing techniques are not abused in the interest of detecting standards, while ignoring defects. Higher usable sensitivity allows detecting more flaws than previously possible, and to enjoy larger clearance factors between the search coil and material with obvious benefits in mechanical reliability. In the past, this clearance factor between search coil and material was one of the principal limitations for in-line inspection. Typical clearances were only of the order of 0.5 mm. The system's mechanical reliability in a factory environment was poor. With modern coil constructions and electronic techniques however, clearances of up to 6.5 mm can be achieved, benefiting overall system reliability. Developments in automatic solid state balance control have virtually eliminated the need for operator supervision, other than for effecting size changes. Long term stability is now measured in years rather than half-hour periods. It is a popular misconception that eddy current testing can detect only surface defects. This is true of rotating probe systems, but when testing tubing with encircling or saddle type coils, ID defects have been detected in 13 mm wall carbon steel and stainless steels. Depth of penetration is the point where the eddy current density has decreased to 37% of its surface value. In magnetically saturated, carbon steel tube, typical penetration depth using a 10 kHz test frequency is around 3 mm. A more recent technique, however, is not to magnetically saturate the material, but simply polarize it. The result is sensitivity to defects at a much greater depth produced by magnetic flux leakage effects on the eddy current flow pattern.

3.1 Defects, which can be detected

The system sensitivity is adjustable to suit individual user requirements. It is usually calibrated to meet approved standards, such as American Society for Testing and Materials (ASTM) or American Petroleum Institute (API). To be detectable, natural defects must produce a disruption of the eddy current flow pattern greater than that produced by the calibration standard. They must also occur within the field of inspection. They may be not visible at the

surface. Typical flaws which can be detected are: *pin-holes, cross cracks, lamination, seam cracks, butt welds, porosity, hook cracks, lack of fusion, edge damage, burned edges, open seams.* The sensitivity is limited by the material's quality. For example, higher sensitivity is possible on cold-rolled rather than hot-rolled material.

3.2 What cannot be detected?

Many defects may be missed by eddy current inspection. For instance, *slight undercut or overcut of scarf, absolute loss of penetration, certain 'pasty' welds, defects occurring outside the field of inspection, brittle welds, signals not exceeding calibration levels, defects created by subsequent processing* will be not detected.

3.3 Eddy current transducers

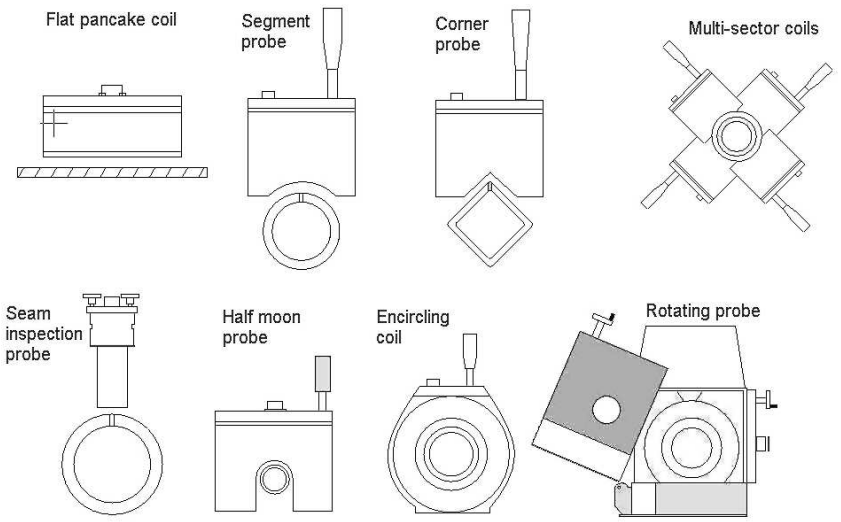

Fig. 13. Eddy-current transducers.

Flat pancake coils: available in discrete sizes with sensing widths up to 25cm. Used to inspect surface of the material.

Seam inspection probes: located on the weld platform to test only the weld seam. With the help of differential detection windings they monitor

weld condition. With absolute windings they enable detection of open seam conditions. One size fits all.

Segment probes: covering effective arc of about 38 mm permits inspection of the quadrant on round tubes

Half moon probes: used for pipes with diameters less than 90 mm. Need to be matched to tube sizes in 5 mm increments.

Corner probes: to check the shapes formed close to the corner.

Encircling coil: must be matched to individual tube diameters. Suitable for small diameter tubes, such as refrigeration, hearing element and cable sheathing.

Multi-sector coils: replaces a series of segment probes conformed in a radial pattern around the tube or pipe.

Rotating probes: enable to check for longitudinal surface cracks.

4 Finite Elements Simulation in Nondestructive Testing of Materials

The theoretical analysis of the electromagnetic field distribution in eddy current systems is very difficult and unsolved at this time. Numerical methods, those of finite elements in particular, offer some new tools for the analysis of eddy- current flaw detection systems. The problem of nonlinearity of the medium and its geometrical form has been solved in the case of two-dimensional and axially symmetric systems, the problem of analysis of three-dimensional systems remaining still unsolved, however. In addition to the difficulties connected with the uniqueness of solution or the way of determining the boundary conditions there is a serious obstacle of limited capacity of the memory and calculation speed of computers.

4.1 The 2-D model of the probe for surface tests

The Förster flaw detector is equipped with a number of probes for testing surfaces. They differ by their dimensions, and the selection of a suitable probe depends on the expected size of the flaw and the quality of the surface to be tested. A sectional view of the model of the Förster-probe is presented in Fig.15. The model is axially symmetric, this fact being made use of only for determining the frequency characteristics of the probe in the case of no flaw being present, however. The probe is composed of a screened coil with a ferromagnetic core. It has been placed on an electrically conducting plate containing a flaw to be detected. In order to reduce the error due to the

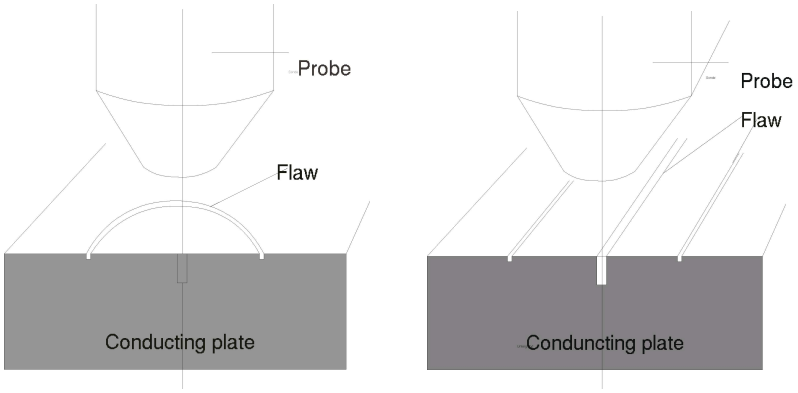

Fig. 14. Cylindrical (left) and Cartesian(right) 2-D models of sensors and cracks.

analyzed region truncation, infinite elements have been introduced on the boundary.

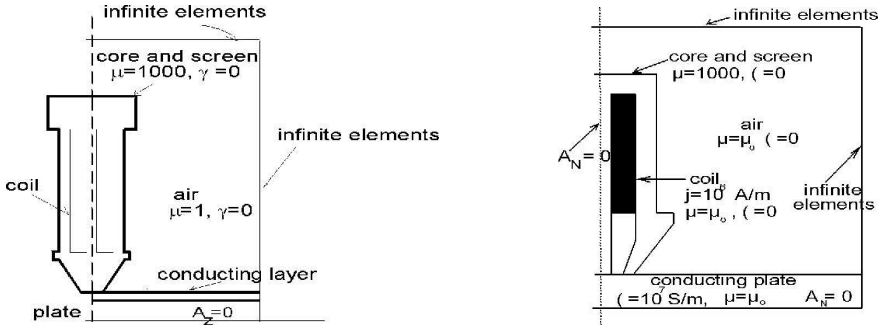

Fig. 15. The models of pencil-probe.

The calculations were performed by the method of finite elements, using the magnetic vector potential $\boldsymbol{A}$ defined as $\boldsymbol{B} = \mathrm{rot}\boldsymbol{A}$. Similarly to the currents generating the magnetic field, this vector potential has only one component, $\boldsymbol{A}_\phi$. The distribution of the potential is described by the equation

$$\frac{\partial}{\partial r}\left[\frac{1}{r\mu}\frac{\partial(A_\phi r)}{\partial r}\right] + \frac{\partial}{\partial z}\left[\frac{1}{r\mu}\frac{\partial(A_\phi r)}{\partial z}\right] = 0 \tag{1}$$

for the air, the core and the screen,

$$\frac{\partial}{\partial r}\left[\frac{1}{r\mu}\frac{\partial(A_\phi r)}{\partial r}\right] + \frac{\partial}{\partial z}\left[\frac{1}{r\mu}\frac{\partial(A_\phi r)}{\partial z}\right] = J_0 \tag{2}$$

for the coil and,

$$\frac{\partial}{\partial r}\Big[\frac{1}{r\mu}\frac{\partial(A_\phi r)}{\partial r}\Big] + \frac{\partial}{\partial z}\Big[\frac{1}{r\mu}\frac{\partial(A_\phi r)}{\partial z}\Big] = j\omega\gamma A_\phi \tag{3}$$

for the conducting plate.

Fig.16 shows the finite element meshes used for analysis. They were obtained by means of a generator on the basis of macro-elements. Next the mesh was subjected to an adaptive process which resulted in considerable mesh refinement inside the conducting plate in the neighborhood of the flaw. The mesh generators and adaptive algorithms are part of the SONMAP-*micro* software package and have been described in [1].

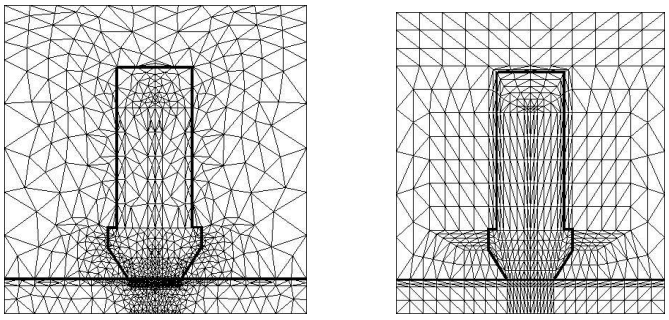

Fig. 16. Finite element meshes for the pencil probe.

The H 2.835 Förster-defectometer analyses only the real part of the probe impedance. To determine the optimum operation frequency of the probe, the frequency characteristics of the probe resistance variation were determined.

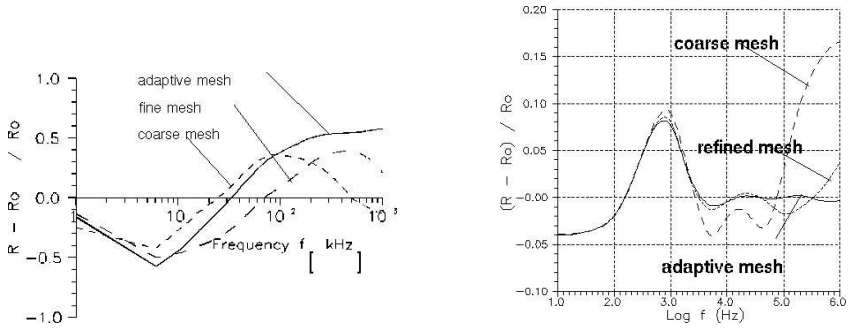

Fig. 17. Frequency characteristics of the pencil probe testing: left - surface crack, right - inner crack.

The left-hand Fig.17 illustrates the frequency characteristics of the probe resistance during the detection for a surface flaw of a depth of 0.5 mm and

a width of 1 mm. The detection sensitivity for such a flaw increases with frequency. It is seen that the results obtained for the fine mesh and the adaptive mesh are, in this case, similar. The frequency characteristics for a flaw detecting below the plate surface is represented in the right-hand figure. The dimensions of the flaw, which was located at a depth of 1 mm below the surface, were 1×1 mm. Such a defect cannot be detected, if the feed frequency of the probe is too high, the advantages of the use of the adaptive method are therefore obvious.

The characteristics presented above have been obtained for a location of the flaw corresponding to the output signal of maximum level. The resistance variations of the probe are obtained during the passage of the probe above the flaw. Their form shows the size and the character of the flaw. Fig.18 shows such characteristics, obtained by simulation, for two frequencies and different element meshes. The defect was located at the surface and its dimensions were not changed.

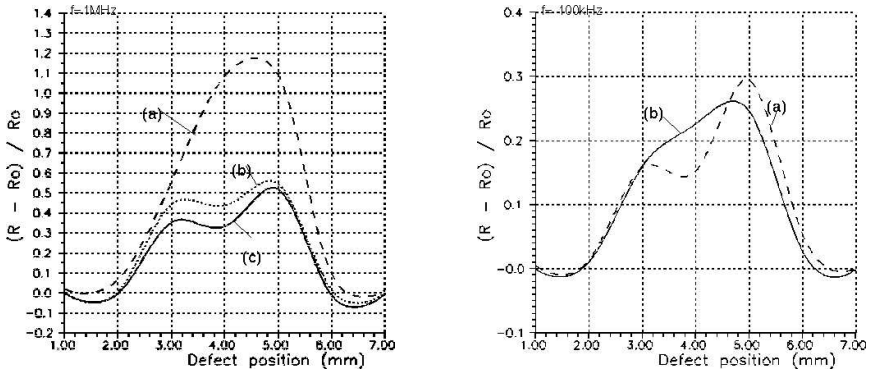

Fig. 18. Relative resistance variation of the probe during passage above the flaw: (a) a mesh of 311 nodes, (b) a mesh of 587 nodes, (c) an adaptive mesh of 497 nodes.

The only fact considered in the analysis presented here is the variation of the probe resistance. It has been shown by computation that the induction reactance dominates the resistance, its variation under influence of the presence of the flaw being insignificant, however. This is due to the fact that the structure of the sensor is such that most of the field lines are closed inside the probe so that they do not pass through the material (Fig.19). The algorithms described enable us to optimize the structure of the sensors.

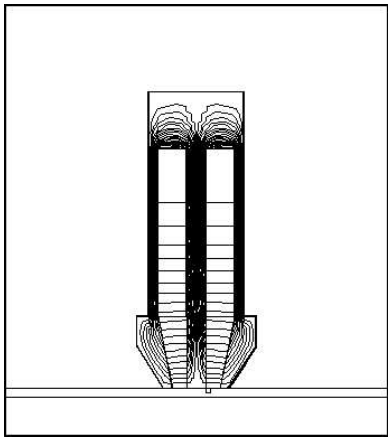

Fig. 19. Field lines of the pencil probe.

4.2 Axisymmetric model for tube testing simulation

The model under investigation is shown in the figure below. It consists of the differential coil inside a tube. The material defect is also shown. This model is adequate to the test sample, which is described by DIN 54141.

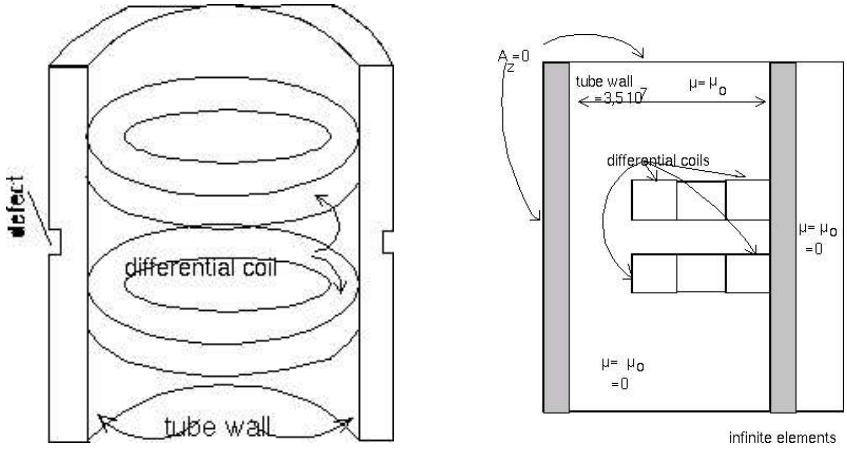

Fig. 20. Differential coils inside of tubes.

The use of the cylindrical two-dimensional models can be a good approximation of three-dimensional problems, as long the coils are not displaced from their central position (Fig.20 right). Similarly to the model of the sensor for surface tests the calculations were provided for the magnetic vector potential A. The feed frequency is low enough and the displacement current

term in Maxwell's equations is negligible. For sinusoidal excitation the eddy current field equations become the form Eq(1), (2) and (3). The flux density lines nearby sensor obtained by FEM are shown in the Fig.21. The feeding frequency is equal to 50kHz.

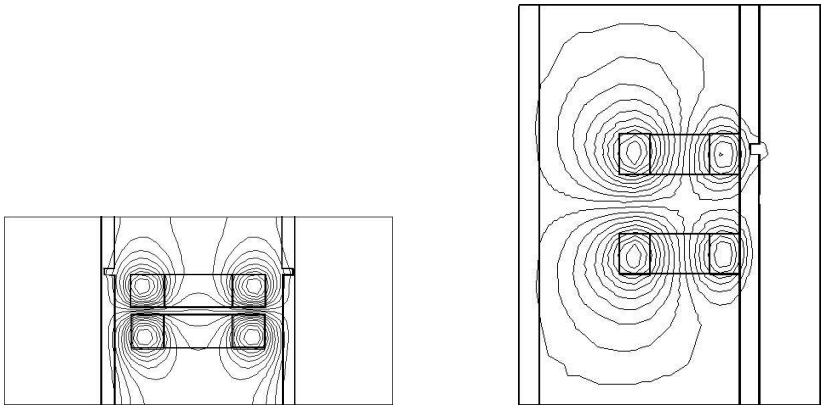

Fig. 21. Field lines of differential coils inside tubes.

For purposes of eddy current testing, the most important feature of the FEM analysis is the ability to compute the impedance Z at the terminals of the sensor with respect to defects. A plot of Z on the complex impedance plane for various positions of the probe as it moves past a defect gives the predicted eddy current probe signal trajectory for that defect. The impedance trajectory can serve as a certificate of the product. The exemplary impedance trajectories for outside and inside defects are shown in the Fig.22 and 23.

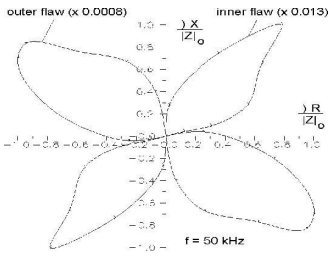

Fig. 22. Impedance trajectories for outside and inside flaws.

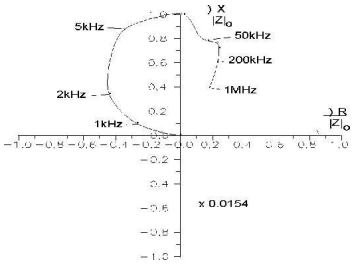

Fig. 23. Impedance variation versus feeding frequency.

The problem of choosing a proper value of frequency is of great importance. The optimal frequency of the input signals depends on the tube wall thickness and defect depth. The output signals for various frequencies and

for arbitrary position of the sensor with respect to the inner defect are shown in the figure below.

4.3 The three-dimensional NDT Model

The structure of a probe of an eddy-current defectometer being axially symmetric, it can easily be described by means of a two-dimensional model. Considerable difficulties arise, however, if material flaws, which are not symmetric, in general, are to be modeled. In this case a three-dimensional model must be used [1]. In addition to the difficulties of mathematical formulation of the problem there are also difficulties of numerical nature, due to he computing power of the existing computers, being too low in the case of analysis of vector fields, in particular. Below, we shall present an idea of determining 3-D fields by means of a scalar function. The analysis will be made by using the magnetic scalar potential φ and the electric vector potential $\boldsymbol{T}$. They are related with the magnetic field intensity vector $\boldsymbol{H}$ and the current density $\boldsymbol{J}$ by the equations

$$\boldsymbol{H} = \boldsymbol{T} - \text{grad } \varphi \tag{4}$$

and

$$\boldsymbol{J} = \text{rot } \boldsymbol{T}. \tag{5}$$

The distribution of the potential $\boldsymbol{T}$ is a known function describing the excitation current density. This method excludes the existence, in the region analyzed, of unknown eddy currents, which cannot be described under such conditions by means of the potential $\boldsymbol{T}$. Since the principle of measurement with Frster-defectometer is based on the interaction of eddy currents with the probe, special impedance boundary conditions may be used to take them into account. The model analyzed is of a relatively simple configuration because it constitutes a rectangular coil located above the conducting plate. A cross-section of this model in the x, y-plane is shown in Fig.24.

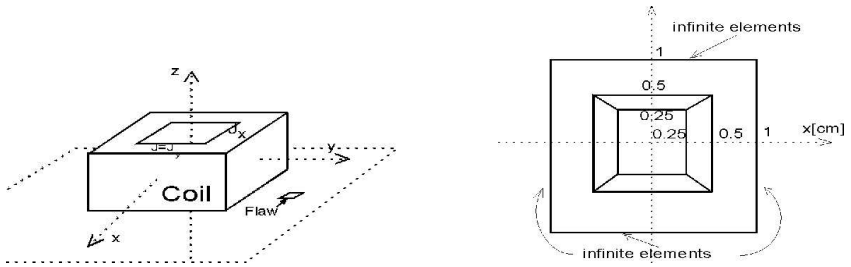

Fig. 24. Rectangular coil above a plate with a flaw and the x, y-section of the model.

A three-dimensional element mesh was obtained by means of layer-generator. It extends the existing triangular mesh in the direction of the third dimension, forming first prisms, then tetrahedrons. The application of tetrahedrons as finite elements has many advantages. The shape functions are simple and may be integrated analytically. It makes possible defining of stiffness matrix coefficients explicit. Next, such a mesh can be refined by means of an adaptive method, as a result of which new tetrahedrons are formed [1]. A drawback of the use of tetrahedron elements is that a considerable number of such elements are needed for a mesh. The initial mesh had 405 nodes and 1536 elements. If the scalar potential φ is used the currents exciting the magnetic field are taking into account by considering the electric potential $\boldsymbol{T}$. The current density in the coil has only two components, J_x and J_y, therefore there is only one component T_z. The potential $\boldsymbol{T}$ exists inside coil only.

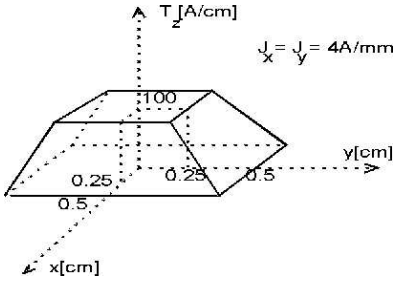

Fig. 25. Definition of the function $\boldsymbol{T}$.

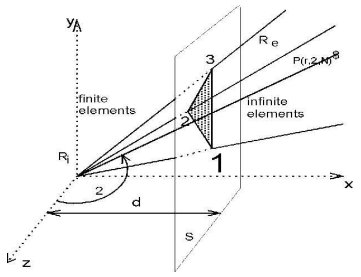

Fig. 26. The idea of infinite elements.

The conducting plate below the coil was taken into account by imposing an impedance condition at the boundary of the region:

$$\frac{\partial \phi}{\partial y} = \kappa\Big(\frac{\partial^2 \phi}{\partial x^2} + \frac{\partial^2 \phi}{\partial z^2}\Big) \tag{6}$$

where $\kappa = \mu_r(1-j)\delta/2$, $\delta = \sqrt{2/(\omega\mu\gamma)}$ and μ_r is relative permeability of the medium.

Taking into account the impedance boundary condition results in the additional terms that are to be introduced into the stiffness matrix of the element.

The model described here has many symmetry planes so that only one-eighth of the region can be taken for computation. The zero Dirichlet-condition was imposed at the $z = 0$ plane and the zero Neumann condition in the remaining planes of symmetry. Because a truncation of the region may be a cause of considerable errors, infinite elements were used [2]. Such

an element, made to suit the tetrahedrons, is shown in Fig.26. If the scalar potential of the magnetic field φ in an infinite element is to decrease in agreement with the imposed function $f(r)$, it suffices to assume for φ the following expression

$$\phi^e(r,\Theta,\varphi) = \frac{f(r)}{f\Big(\dfrac{d}{\sin\Theta\cos\varphi}\Big)} \sum_{i=1}^{3} N_i\phi_i \tag{7}$$

with the classical shape functions for triangular elements, N_i. For the function $f(r)$ we assume, in the simplest case, $f(r) = 1/r^n$, $n \geq 1$. Then, the coefficients of the matrix can be determined by analytical means.

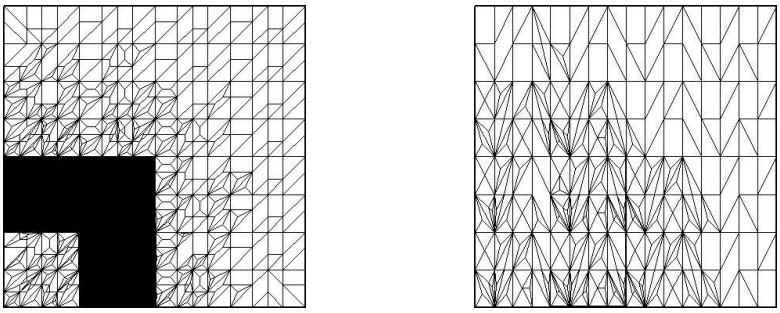

Fig. 27. Sections of 3D finite element tetrahedron meshes.

Fig.27 presents sections of element meshes which were used for computation (1400 nodes), showing mesh refinement obtained by adaptive methods. Those meshes were used for simulating the detection of a surface flaw. The flaw was modeled by a rectangle of the dimensions - 0.125×0.125cm. It was assumed that the magnetic field is perpendicular to the plate surface at the rectangle modeling the flaw. This assumption was realized by means of the impedance boundary condition with the parameters $\mu_r = 1000$ and $\gamma = 1$S/m. The flaw was translated along the x-axis of the probe by steps of 0.125cm, the number of which was eight. Relative variations of the coil resistance for different locations of the flaw are shown in Fig.28.

The simulation process was carried out with two frequencies, namely those of 1kHz and 100kHz. It should be stressed that the impedance boundary condition works correctly by small penetration depth of the field, which means high frequencies. The tests which were performed showed that there was agreement within the limits of 10% with other methods of power losses analysis in the conducting material by solving the Helmholtz equation.

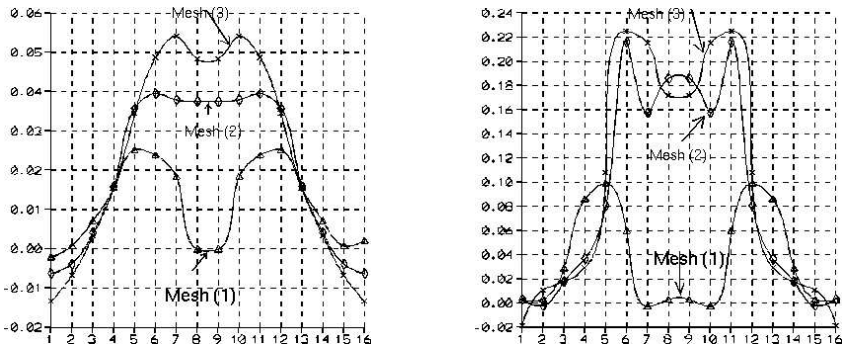

Fig. 28. Relative variation of coil resistance for three meshes: (1) - initial mesh, (2) - fine mesh, (3) - adaptive mesh, f=100kHz.

5 Sensitivity Analysis of Electromagnetic Quantities with FEM

Sensitivity analysis belongs to the most important tools in optimization theory. For several objective functions the sensitivity may be directly calculated differentiating the objective function versus one of material or geometric parameters. For the tasks based on local quantities the direct calculation is also possible, but it requires very large computational effort. A number of well described sensitivity evaluation methods exist in electric circuit theory [5]. These methods could be adapted to electromagnetic field analysis programs, too. The first one bases on a version of Tellegen's theorem for electromagnetic field theory. This method allows to calculate the sensitivity of chosen local quantities, as magnetic vector potential, impedance of a coil or induced voltage, versus material parameters in a whole region at once. The second method bases on differentiation of stiffness matrix of finite elements. The stiffness matrix contains complete information about geometric and material properties of the model. On the contrary to Tellegen's method, this method allows to calculate the sensitivity of all local quantities versus only one chosen parameter.

5.1 Recognition of electrical conductivity distribution basing on sensitivity information

The task of conductivity recognition may be used for identification of crack shape [6]. When using the eddy- current defectometer, the user should determine the search region, where the crack shape will be recognized. Then, the user should carry out the sufficient number of measurements of flux density

around the crack. The number of measurements depends on discretization of the search region in finite elements. The discretization should be fine enough for modeling shape of the crack. To obtain the proper inverse job, the number of measurement points has to be equal to the number of finite elements in search region. The dependence between conductivity γ inside of finite elements and the field distribution over conducting plate represented by the magnetic vector potential $\boldsymbol{R}$, is given by the following equation

$$\begin{bmatrix} \Delta R_1 \\ \Delta R_2 \\ \Delta R_3 \\ \vdots \\ \Delta R_j \end{bmatrix} = \begin{bmatrix} S_{11} & S_{12} & S_{13} & \dots & S_{1i} \\ S_{21} & S_{22} & S_{23} & \dots & S_{2i} \\ S_{21} & S_{32} & S_{33} & \dots & S_{3i} \\ \vdots & \vdots & \vdots & \vdots & \vdots \\ S_{j1} & S_{j2} & S_{j3} & \dots & S_{ji} \end{bmatrix} \begin{bmatrix} \Delta\gamma_1 \\ \Delta\gamma_2 \\ \Delta\gamma_3 \\ \vdots \\ \Delta\gamma_i \end{bmatrix} \tag{8}$$

where j is number of measurement points, i is number of elements in the search region, $[\boldsymbol{S}]$ is sensitivity matrix. The field measurements can be carried out with constant feeding frequency ω. However, when identifying an inner crack, the multi- frequency method can be used. In both cases, the sensitivity values S_{ji} are evaluated in frequency domain. If the eddy- currents are induced by the coil driven with non-harmonic current impulse, the time-domain evaluation is necessary.

The objective function in the conductivity recognition problems is nonlinear to material conductivity. So the iterative procedure of mathematical programming using sensitivity information has to be adopted. For the examples shown below, the gradient method was chosen. After each iteration the results are compared with that of measurements and the new ΔR_j values for Eq.(6) are obtained. The described methods require access to the source code of finite element package. However, the obtained algorithms are very effective.

5.2 Tellegen's method

The Tellegen's method requires an additional term $\boldsymbol{L}_0$ in Maxwell's equations:

$$\mathrm{rot}\boldsymbol{E} = -\boldsymbol{L}_0 - \mathrm{j}\omega\boldsymbol{H} \tag{9}$$

and

$$\mathrm{rot}\boldsymbol{H} = \boldsymbol{J}_0 + (\gamma + \mathrm{j}\omega\varepsilon)\boldsymbol{E}_0, \tag{10}$$

$\boldsymbol{L}_0$ can be interpreted as a magnetic current density. It should be equal zero in every physical system, but the adjoint system may be non-physical.

Applying the divergence theorem sensitivity equation may be derived [6,7]

$$\int_V (\boldsymbol{J}_0^+ \Delta \boldsymbol{E} - \boldsymbol{L}_0^+ \Delta \boldsymbol{H}) \mathrm{dV} = \int_V (\boldsymbol{E}\boldsymbol{E}^+ \Delta\gamma + j\omega \boldsymbol{E}\boldsymbol{E}^+ \Delta\varepsilon - j\omega \boldsymbol{H}\boldsymbol{H}^+ \Delta\mu) \mathrm{dV} + \int_S (\boldsymbol{H} \times \Delta \boldsymbol{E} + \boldsymbol{E}^+ \times \Delta \boldsymbol{H}) \boldsymbol{n} \mathrm{dS} \tag{11}$$

Above equation determines how to construct the adjoint model. The excitation current $\boldsymbol{J}_0^+$ should be driven into this node, where the sensitivity value of $\boldsymbol{E}$ has to be obtained. Similar, the magnetic current $\boldsymbol{L}_0^+$ makes possible sensitivity calculation of $\boldsymbol{H}$. The proper boundary conditions of both systems cause vanishing of surface integral in Eq.(11). It means, the original and adjoint systems differ only in excitations and boundary conditions. The geometrical properties and material parameters are the same. Further, the stiffness matrix of both systems is the same and requires the factorization only once.

5.3 Method of stiffness matrix derivative

This method was described in the paper [6]. The stiffness matrix $[\boldsymbol{A}]$ is computed in every finite element code

$$[\boldsymbol{A}][\boldsymbol{R}] = [\boldsymbol{b}] \tag{12}$$

Variation of electric conductivity γ of the material causes such changes of potentials vector $[\boldsymbol{R}]$ that the excitation vector remains unchanged

$$\frac{\partial}{\partial x}[\boldsymbol{A}][\boldsymbol{R}] + [\boldsymbol{A}]\frac{\partial}{\partial x}[\boldsymbol{R}] = [\boldsymbol{0}] \tag{13}$$

This formula allows to formulate the nodal sensitivity versus conductivity γ

$$[\boldsymbol{S}] = \frac{\partial}{\partial x}[\boldsymbol{R}] = -[\boldsymbol{A}]^{-1}\frac{\partial}{\partial x}[\boldsymbol{A}][\boldsymbol{R}] \tag{14}$$

In numerical implementation the sensitivity is calculated on the basis of equation system Eq.(13). Unlike to Tellegen's method in this method the sensitivity of all nodal potentials versus conductivity in one finite element is obtained. To calculate the sensitivity for other element the derivative of stiffness matrix should be determined anew. The terms of stiffness matrix are linear functions of electrical conductivity γ, so the matrix of derivatives contains only constants and zeroes.

Assuming the same number of finite elements and the nodes, for which the sensitivity is obtained, both methods seem to be equivalent in calculation time. As result of both methods the sensitivity matrix is obtained. The matrix is necessary to solve linear equations system Eq.(8).

5.4 Recognition of crack shape in conducting plates

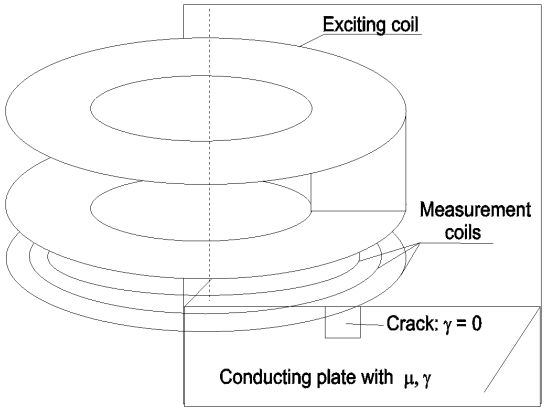

Fig. 29. Crack recognition in a conducting plate.

A measurement of magnetic flux over conducting boundary allows to determine the conductivity distribution inside the material. For instance, a magnetic flux was measured by j measuring coils (Fig.29). The voltage induced in the coils is proportional to the magnetic flux. If we describe the field with the help of a magnetic vector potential, the flux is proportional to the value of $\boldsymbol{R}$ at this point. Let us assume, that the area of interest is discretized by i finite elements. The conductivity changes of those elements are related to the nodal potentials by the sensitivity matrix (Eq.8). A very convenient case is when $i = j$. Then, one can treat Eq.(8) as a system of equations with unknown values of conductivity changes $\Delta\gamma_i$. The recognition process is carried out in an iterative manner. At every step, conductivity values γ_i within the search area are corrected using $\Delta\gamma_i$, computed from Eq.(8). The described algorithm works well for cracks on the outer boundary of a conducting plate. In case of a crack inside the plate, the system of equations Eq.(8) may be ill-conditioned and its matrix close to being singular. The problem can be better posed adopting the Tikhonov

regularization

$$\begin{aligned} S^*_{kk} &= S_{kk} + \alpha \\ S^*_{kk} &= \sum_{m=1}^{i} S_{mk} S_{ml}, \quad \text{and} \\ \Delta R^*_k &= \sum_{m=1}^{i} S_{mk} \Delta R_m \end{aligned} \tag{15}$$

The regularization parameter a is selected automatically to assure the value of matrix determinant about 0.001. An improvement in the conditioning of the equations system can be also achieved by flux measurement at many different frequencies.

Fig.30 presents recognized conductivity distribution near two cracks on the face of a conducting plate. This distribution was achieved after four iterations. In Fig.31, one can see the crack inside of a conducting region, placed oblique to the face. Experimental recognition of such a crack is possible only when using the multi-frequency method. The same problem is present in numerical simulations, thus the measurement was carried out for two supplying frequencies: 1Hz and 100Hz. In the other case, the matrix $[\boldsymbol{S}]$ was singular and the regularization was not sufficient. The conductivity distribution shown in Fig.31 was obtained after ten iterations.

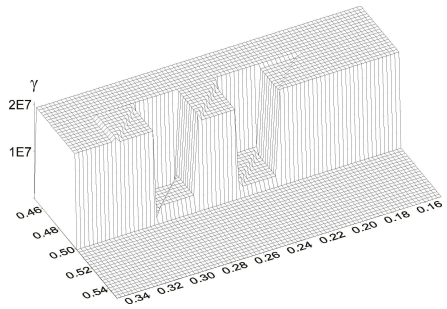

Fig. 30. Recognition of two cracks on the surface.

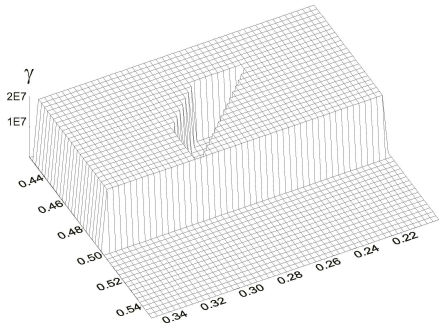

Fig. 31. Recognition of an inner crack.

6 Conclusions

The success of a numeric recognition of conductivity distribution depends mainly on the exact measurement of the magnetic flux. The error of sensitivity evaluation has secondary meaning and influences only the manner in

which the result is obtained. In the examples shown above, instead of the measurements the models with cracks were analyzed with an FEM providing data for further iterative process. Then, the cracks were removed, and the algorithm tried to reconstruct the nodal potentials based on sensitivity values of the nodes. When using the real data containing measurement errors the results could be worse.

References

[1] K. M. Gawrylczyk: *Adaptiven Algorithmen auf der Basis der Methode der Finiten Elemente*, Wyd. Naukowe Politechniki Szczecinskiej, Szczecin, 1992.

[2] S. Gratkowski, K. M. Gawrylczyk: *A Simple Infinite Element for 3-D open boundary magnetic field analysis*, 5th IGTE Symp. Sept.28-30, 1992, Graz, Austria, pp.145-149.

[3] WWW-pages of Förster-group: `www.foerstergroup.de`

[4] Technical information of Prüftechnik GmbH *Eddy current testing finds tube faults*, by Brian Roberts, September 1999 issue of Forming & Fabricating.

[5] L. O. Chua, P. M. Lin: *Computer-Aided Analysis of Electronic Circuits*, Prentice-Hall, New Jersey, USA.

[6] K. M. Gawrylczyk: *Sensitivity evaluation methods of electromagnetic quantities with FE-analysis*, COMPEL, Vol.17, No 1/2/3,1998, pp.78-84.

[7] D. N. Dyck, D. A. Lowther, E.M. Freeman: *A Method of Computing the Sensitivity of Electromagnetic Quantities to Changes in Materials and Sources*, IEEE Trans. on Magnetics, vol.30, No.5, Sept. 1994, pp.3415-3418.